Full gravity gradient tensor of a vertical pyramid model of flat top & bottom with depth-wise parabolic density variation

Anand P. Gokula and Rambhatla G. Sastry, Department of Earth Sciences, Indian Institute of Technology Roorkee, Email ID: rgssastry@gmail.com / rgss1fes@iitr.ac.in.

Keywords

Gravity gradient tensor, vertical pyramid model, right rectangular prism, parabolic density function.

Summary

Gravity gradient tensor and their different types of combination are very useful to delineate the edges of the source body. It enhances the high frequency gravity anomalies and outlines the shape of the anomalous body. Full gravity gradient tensor and their interpretation for right rectangular prism and polyhedral body are present in geophysical literature. Here, we propose a vertical pyramid model with parabolic density function and their gravity gradient tensor. These gravity gradient tensors expressions are validated against that of right rectangular prism model. We have included two synthetic examples - A symmetric pyramid model and right rectangular prism model (made by two pyramid models) and tried to delineate the edges of the source body. These preliminary results are very encouraging and can be applied for delineation of sedimentary basins in greter detail in future.

1. Introduction

The use of gravity gradient data is more common in exploration and is widely used to delineate the outline of the source body. Gravity gradient tensors are present in geophysical literature for right rectangular prism with constant density as well as linear density variations. Complete gravity gradient tensor can also derive from the vertical component of the gravity using Fast Fourier transform techniques (Mickus and Hinojosa, 2001). Different types of density function, like exponential (Chai and Hinze 1988), parabolic (Rao *et al.* 1993; Chakravarthi *et al.* 2002) and hyperbolic density functions (Rao *et al.* 1995) have been used in sedimentary basin modelling. Hansen (1999), Holstein (2003) and Hamayun *et al.* (2009) have used polyhedral model in gravity forward modelling with a linear density variation depth-wise.

Gravity gradient tensors are useful to estimate the source location and edge detection of source body (Blakely, 1986; Zeng, 2002; Boschetti, 2005; Beiki, 2010; Beiki and Pedersen, 2010, Zuo, 2015). Saad, (2006), demonstrates the complex pattern of the anomalies of salt domes, starting from the gravitational potential to the full gravity gradient tensors and their combinations. The detailed study of singularities encountered in gravity forward modelling of different models has been addressed by Okabe (1979), Pohanka (1988),Kwok (1991), Petrović (1996), Tsoulis (2000), Tsoulis and Petrović (2001), Holstein (2002) and D'Urso (2013).

Starostenko(1978) has proposed an inhomogeneous vertical pyramid model of flat top and bottom with linear density variation depth-wise. But he was unable to derive the complete analytical expressions for its full gravity gradient tensor.

We derived the complete analytical expressions of full gravity gradient tensors of the pyramid model, but not included due to page limitation. We have plotted all gravity gradient tensors and their different gravity gradient combinations to delineate the edges of the source body (synthetic pyramid model).

2. Theory

Consider an isolated regular pyramid model with depth-wise parabolic density contrast, ABCDEFGH with flat top, ABCD and bottom surface, EFGH (Fig. 1). The potential effect of such a model at any arbitrary point (x, y, z) in free-space is given by,

$$U(x,y,z) = ¥ \int_{,=h_1}^{h_2} \int_{¦=¦_l}^{¦_u} \int_{¶=¶_l}^{¶_u} \frac{\Delta°(,)d¶d¦d,}{\sqrt{(¶-x)^2+(¦-y)^2+(,-z)^2}} \quad (1)$$

where, parabolic density contrast, Δρ (ζ) and limit of variables ξ and η are given by,

$$\left.\begin{aligned}
&\Delta\rho(\zeta)=\Delta\rho_0/\left[\Delta\rho_0-\alpha(\zeta-h_1)\right]^2\\
&\rho_l=(h_1-\zeta)(\rho_1-\rho_3)/(h_2-h_1)+\rho_1,\\
&\rho_u=(h_1-\zeta)(\rho_2-\rho_4)/(h_2-h_1)+\rho_2,\\
&\eta_l=(h_1-\zeta)(\eta_1-\eta_3)/(h_2-h_1)+\eta_1 \;and\\
&\eta_u=(h_1-\zeta)(\eta_2-\eta_4)/(h_2-h_1)+\eta_2.
\end{aligned}\right\} \quad (2)$$

where, γ is the universal gravitational constant, Δρ is the density contrast observed at the ground surface in g/cm^3, α is a parabolic density function in g/cm^3/km, h_1 and h_2 are the depth of the top and bottom surface of the pyramid and ζ refers to depth below h_1. The value of α can be obtained by fitting parabolic density function (first one of equation 2) to the known density contrast-depth data of sedimentary rocks (Chakravarthi *et al.* 2002). A(ξ_1,η_1,h_1), B(ξ_1,η_2,h_1), C(ξ_2,η_2,h_1), D(ξ_2,η_1,h_1),E(ξ_3,η_3,h_2), F(ξ_3,η_4,h_2), G(ξ_4,η_4,h_2) and H(ξ_3,η_3,h_2) are corners of the pyramid (Fig. 1). By changing the variables on the right hand side (RHS) in equations (1) and (2),

$$\rho-x=\rho',\quad \eta-y=\eta' \quad and \quad \zeta-z=\zeta',$$

we get,

$$U(x,y,z)=\gamma\int_{\zeta'=h_1-x}^{h_2-x}\int_{\eta'=\eta_l-y}^{\eta_u-y}\int_{\rho'=\rho_l-x}^{\rho_u-x}\frac{\Delta\rho(\zeta')\,d\rho'\,d\eta'\,d\zeta'}{R} \quad (3)$$

Where,

$$\left.\begin{aligned}
&\Delta\rho(\zeta')=\Delta\rho_0/\left[\Delta\rho_0-\alpha(\zeta'+z-h_1)\right],\\
&\rho_l'=(h_1-\zeta')(\rho_1-\rho_3)/(h_2-h_1)+\rho_1,\\
&\rho_u'=(h_1-\zeta')(\rho_2-\rho_4)/(h_2-h_1)+\rho_2,\\
&\eta_l'=(h_1-\zeta')(\eta_1-\eta_3)/(h_2-h_1)+\eta_1,\\
&\eta_u'=(h_1-\zeta')(\eta_2-\eta_4)/(h_2-h_1)+\eta_2 \;and\\
&R=\sqrt{\rho'^2+\eta'^2+\zeta'^2}.
\end{aligned}\right\} \quad (4)$$

We can rewrite the parabolic density function Δρ (ζ') and the limits ρ' and η' of equation (3) as,

$$\left.\begin{aligned}
&\Delta\rho(\zeta')=\Delta\rho_0/\left[r-\alpha\zeta'\right],\\
&r=\Delta\rho_0-(z-h_1)\\
&\rho'=\rho_l'-x=m_1\zeta'+c_1,\\
&\rho'=\rho_u'-x=m_2\zeta'+c_2,\\
&\eta'=\rho_l'-x=m_3\zeta'+c_3 \;and\\
&\eta'=\rho_u'-x=m_4\zeta'+c_4.
\end{aligned}\right\} \quad (5)$$

where,

$$\left.\begin{aligned}
&m_1=(\rho_3-\rho_1)/(h_2-h_1),\quad m_2=(\rho_4-\rho_2)/(h_2-h_1),\\
&m_3=(\eta_3-\eta_1)/(h_2-h_1),\quad m_4=(\eta_4-\eta_2)/(h_2-h_1),\\
&c_1=(h_1-z)(\rho_1-\rho_3)/(h_2-h_1)+\rho_1-x,\\
&c_2=(h_1-z)(\rho_2-\rho_4)/(h_2-h_1)+\rho_2-x,\\
&c_3=(h_1-z)(\eta_1-\eta_3)/(h_2-h_1)+\eta_1-y \;and\\
&c_4=(h_1-z)(\eta_2-\eta_4)/(h_2-h_1)+\eta_2-y
\end{aligned}\right\} \quad (6)$$

All the gravity gradient components are computed by taking all the possible double derivatives of the potential (equation 3) in x, y and z-direction. So, there are total nine gravity gradient tensors, out of which five are independent (U_{xx}, U_{xy}, U_{xz}, $U_{yy}$and U_{yz}) and four are dependent (U_{yx}, U_{zx}, $U_{zy}$and U_{zz}) gravity gradient tensors. Expressions for all independent gravity gradients in integral form are given below:

$$U_{xx}=-\gamma\Delta\rho_0\int_{h_1-z}^{h_2-z}\left[1/\left(r-\alpha\zeta'\right)^2\right]\left\{\rho'\eta'/\left[(\rho'^2+\zeta'^2)R\right]\right\}_{\rho_l'-x}^{\rho_u'-x}\Big|_{\eta_l'-x}^{\eta_u'-x}d\zeta' \quad (7)$$

$$U_{xy}=\gamma\Delta\rho_0\int_{h_1-z}^{h_2-z}\left[1/\left(r-\alpha\zeta'\right)^2\right]\left[1/\sqrt{\rho'^2+\eta'^2+\zeta'^2}\right]_{\rho_l'-x}^{\rho_u'-x}\Big|_{\eta_l'-x}^{\eta_u'-x}d\zeta' \quad (8)$$

$$U_{xz}=-\gamma\Delta\rho_0\int_{h_1-z}^{h_2-z}\left[1/\left(r-\alpha\zeta'\right)^2\right]\left\{\rho'\zeta'/\left[(\rho'^2+\zeta'^2)R\right]\right\}_{\rho_l'-x}^{\rho_u'-x}\Big|_{\eta_l'-x}^{\eta_u'-x}d\zeta' \quad (9)$$

$$U_{yy}=-\gamma\Delta\rho_0\int_{h_1-z}^{h_2-z}\left[1/\left(r-\alpha\zeta'\right)^2\right]\left\{\eta'\zeta'/\left[(\eta'^2+\zeta'^2)R\right]\right\}_{\rho_l'-x}^{\rho_u'-x}\Big|_{\eta_l'-x}^{\eta_u'-x}d\zeta' \quad (10)$$

$$U_{yz}=-\gamma\Delta\rho_0\int_{h_1-z}^{h_2-z}\left[1/\left(r-\alpha\zeta'\right)^2\right]\left\{\eta'\zeta'/\left[(\eta'^2+\zeta'^2)R\right]\right\}_{\rho_l'-x}^{\rho_u'-x}\Big|_{\eta_l'-x}^{\eta_u'-x}d\zeta' \quad (11)$$

The dependent gravity tensors can be obtained by the symmetric characteristics of the second derivatives (U_{yx}= U_{xy}, U_{zx} = U_{xz} and U_{zy} = U_{yz}) and using the Laplace equation (U_{zz}= -U_{xx} -U_{yy}).

Figure (1) shows a 3-D pyramid model and its geometry with a depth-wise parabolic density variation. Figure (2) shows the complete gravity gradient tensor plots of vertical pyramid along with five independent (U_{xx}, U_{xy}, U_{xz}, U_{yy} and U_{yz}) and four dependent (U_{yx}, U_{zx}, U_{zy} and U_{zz}) gravity gradient tensor. U_{yx}, U_{zx} and U_{zy} are plotted

by symmetric characteristics of the gravity gradient tensor ($U_{yx}= U_{xy}$, $U_{zx} = U_{xz}$ and $U_{zy} = U_{yz}$). A second vertical derivative, U_{zz} is derived from Laplace equation ($U_{zz}= -U_{xx} -U_{yy}$).

Different combinations of gravity gradient components are used in gravity gradient interpretation to simplify their complex pattern (Saad, 2006). Differential curvature or horizontal directive tendency (HDT) of the pyramid model with parabolic density function is computed by the combination of U_{xx}, U_{yy} and U_{xy}.

Differential curvature magnitude (DCM) =

$$\left[\left(U_{xx}-U_{yy}\right)^2+\left(2U_{xy}\right)^2\right]^{1/2} \quad (12)$$

Horizontal and total gradient magnitude of $U_z$of pyramid model is the combination of U_{zx}, U_{zy} and U_{zz}, which are given below:

Horizontal gradient magnitude of U_z (HGM) =

$$\left(U_{zx}^2+U_{zy}^2\right)^{1/2} \quad (13)$$

Total gradient magnitude of U_z (TGM) =

$$\left(U_{zx}^2+U_{zy}^2+U_{zz}^2\right)^{1/2} \quad (14)$$

All these combinations greatly enhance the effect of the shallower sources.

3. Results and discussion

Figure 1 shows our 3-D vertical pyramid model with depth-wise parabolic density variation. We have shown plots of all gravity gradient tensors (Fig. 2) and their combined effects (Fig. 2) for a pyramid model with parabolic density function, which serves as first synthetic example. White dashed and the black solid lines indicate the top and bottom surface of the pyramid model respectively (Fig. 2). Gravity gradient tensors (Fig. 3a) for right rectangular prism (made by two pyramid model, solid black line and dashed white line show the first and second pyramid model) serve as a second synthetic example for the pyramid model with constant density, which is also used for validation purpose.

3.1 Validation

To validate our gravity gradient tensors for a pyramid model, we have considered gravity gradient tensors of a single vertical prism (Fig. 3a) of constant density (Nagy et al., 2000) in the absence of computable gravity for vertical prism model with parabolic density function. We have converted parabolic density function for the pyramid model into constant density by considering α = 0. We have constituted a single vertical prism, equivalent to Nagy et al., (2000) by the combination of the two pyramid model with constant density (Fig. 3b).

Accordingly, Fig. 3a corresponds to the gravity gradient tensors of a vertical prism model of constant density (Nagy et al., 2000) while Figure 3b corresponds to that of our constituted vertical prism model (by the combination of two pyramid model with constant density, shown by solid black and dashed white line respectively in Fig. 3b). Our model response matches well (RMS error of $7.1*10^{-3}$mgal) with that of a vertical prism model.

3.2 Discussion

The complete gravity gradient tensor and their anomaly response plots (Fig. 2 and 3) along with different combinations of gravity gradients (Fig. 2) are used to delineate the edges of a 3-D pyramid model with parabolic density function and right rectangular prism (made by o pyramid models) with constant density.

The white dashed line shows the upper rectangular surface and black solid line show the bottom rectangular surface of the vertical pyramid model (Fig. 2). U_{xx} plot (Fig. 2), shows the positive-negative-positive triplet pattern with strong negative at the centre. The zero contours define the west-east edges of the upper rectangular surface and the positive peaks on both sides of the negative peak define the west-east edges of the lower rectangular surface of the pyramid model along the x-axis. Similarly the U_{yy} plot (Fig. 2), defines the south-north edges of the upper and the lower rectangular surface of the vertical pyramid model along the y-axis. Both the plots, U_{xy} and U_{yx} (Fig. 2) exhibit the negative-positive-negative-positive quadruplet pattern, which exactly define the upper four corners of the vertical pyramid model but not define the bottom corners.

Plots of U_{xz} and U_{zx} (Fig. 2) are same due to the symmetric characteristics of the gravity gradient tensor and similar for U_{yz} and U_{zy} (Fig. 2a). U_{xz} and U_{yz} (Fig. 2) define the west-east and south-north edges of the upper rectangular surface of the pyramid along the x-axis and y-axis respectively, but do not give the information about the lower edges (Fig. 2). The upper rectangular surface inferred by U_{xz} and U_{yz} are similar to that of U_{xx} and U_{yy} (Fig. 2).

U_{zz} is computed via U_{xx} and U_{yy} by using the Laplace equation in source-free region. U_{zz} can be used to define the centre of the pyramid model.

Figure 2 also shows the anomaly plot of differential curvature magnitude, which correctly delineates the edges of the upper rectangular surface but not exactly

delineate the bottom rectangular surface of the vertical pyramid model. All of the four corners of the upper rectangular surface pass though the peak points of the anomaly. Horizontal and total gravity gradients magnitude (Fig. 2) are computed by the combination of the U_{zx}, U_{zy} and U_{zz} and mainly used as an edge detector of the anomalous source. Both horizontal and total gravity gradients delineate the outline of the upper rectangular surface of the vertical pyramid model (edges are passing thorough the peak values), but fail to delineate bottom surface of the pyramid model.

Similar procedure is applied to detect the edges of right rectangular prism model. The edges of the bottom rectangular surface of the right rectangular prism are the same as the edges of the upper rectangular surface, so there are no difficulties to detect the bottom edges of the right rectangular prism model

4. Conclusions

Here, we have undertaken a vertical pyramid model with parabolic density function and derived closed form expression of all the gravity gradient tensor quantities, but due to page limitation, we have shown expressions only in integral form. All the gravity gradient plots (Fig. 2) of vertical pyramid show the complex pattern (single, doublet, triplet and quadruplet) except U_{zz} (monopolar). We have delineated the edges of the upper rectangular surface of the vertical pyramid model with the help of different gravity gradient plots, because of the enhancement of the shallow surface features. Slight positive peaks of the U_{xx} and U_{yy} (Fig. 2) give the information about edges of the rectangular bottom surface of the vertical pyramid.

Different combinations of the gravity gradients like differential curvature magnitude, horizontal gradient magnitude and total gradient magnitude of U_z (Fig. 2) emphasize the effect of the shallow sources and can be used as an edge detector of the anomalous source like our pyramid model.

Our gravity gradients plots for right rectangular prism (made by two pyramid models) match well with that of right rectangular prism model (Nagy et al., 2000) at validation stage.

So, it is easy tooutline the upper rectangular surface of the vertical pyramid model and that of right rectangular prism model, but it is very difficult to delineate the bottom surface.

Acknowledgements

The first author gratefully acknowledges the financial help received from MHRD, Government of India, Delhi.

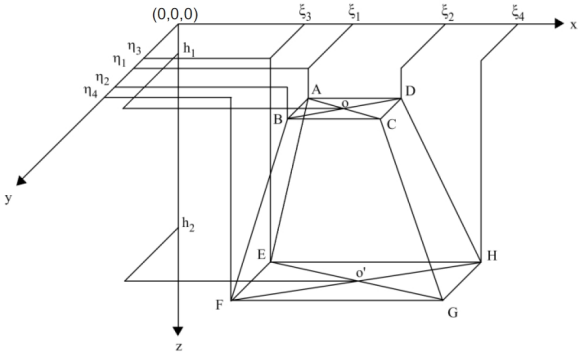

Figure 1.A schematic 3-D pyramid model and its geometry with depth-wise parabolic density variation.

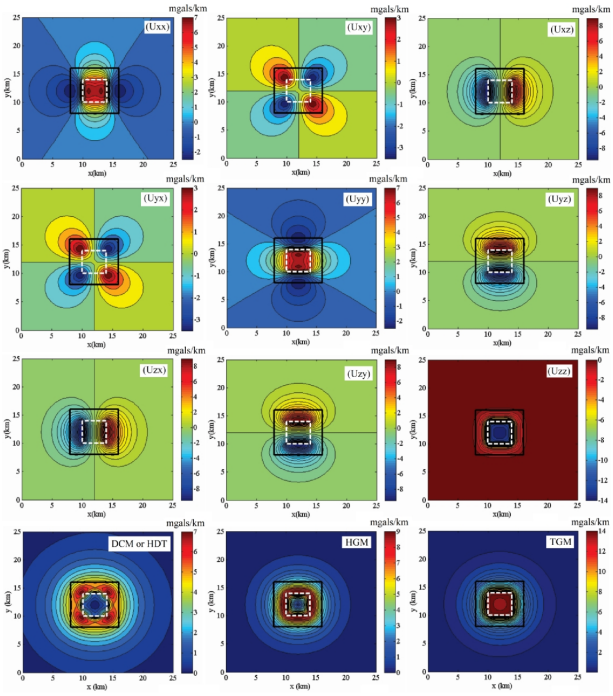

Figure 2. The full gravity gradient tensor and their different combinations of pyramid model with parabolic density function. The parameters of the pyramid model for all cases are as follows: ξ_1 =10, ξ_2 =14, ξ_3 =8, ξ_4 =16, η_1 =10, η_2 =14, η_3 =8, η_4 =16, $\Delta\rho_0$ = -0.5206 g/cm3, α = 0.0403g/cm^3/km, h_1 = 0.5, h_2 = 5 and z = 0. All length parameters and station distances are expressed in km.

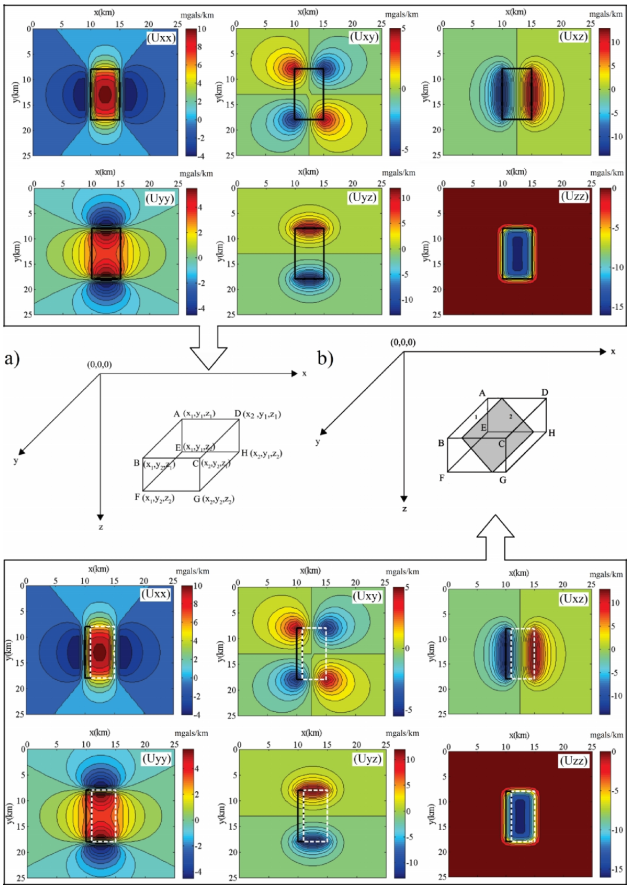

Figure 3. Validation of our gravity gradient tensors for pyramid model with that of right rectangular prism model. a) Gravity gradient tensors for right rectangular prism (Nagy et al., 2000). The parameters of the right rectangular prism model for all cases are as follows: x_1 =10, x_2 =15, y_1 =10, y_2 =15, ρ = -0.5206 g/cm^3, z_1 = 0.5 and z_2 = 5. All length parameters and station distances are expressed in km. b) Gravity gradient tensors for right rectangular prism made by the combination of the two pyramid models. The parameters of the pyramid model for all cases are as follows: ξ_1 =10, ξ_2 =15, ξ_3 =8, ξ_4 =18, η_1 =10, η_2 =15, η_3 =8, η_4 =18, $\Delta\rho_0$ = -0.5206 g/cm3, α = 0 g/cm^3/km, h_1 = 0.5, h_2 = 5 and z = 0. All length parameters and station distances are expressed in km.

Selected References

Barnes, G., and J. Lumley, (2011), Processing gravity gradient data, Geophysics, 76, I33–I47, doi: 10.1190/1.3548548

Beiki, M., (2010), Analytic signals of gravity gradient tensor and their application to estimate source location, Geophysics, 75, I59–I74, doi: 10.1190/1.3493639.

Beiki, M., and L. B. Pedersen, (2010), Eigenvector analysis of gravity gradient tensor to locate geologic bodies, Geophysics, 75, I37–I49, doi: 10.1190/1.3484098

Blakely, R. J., and R. W. Simpson, (1986), Approximating edges of source bodies from magnetic or gravity anomalies, Geophysics, 51, 1494- 1498.

Eckhardt, E. A., (1940), A brief history of the gravity method of prospecting for oil Geophysics, 5, 231–242.

Eshagh, M., and L. E. Sjoberg, (2009), Atmospheric effects on satellite gravity gradiometry data, Journal of Geodynamics, 9–19, doi:10.1016/j.jog.2008.06.001.

Mickus,K. L., and J. H. Hinojosa, (2001), The complete gravity gradient tensor derived from the vertical component of gravity: a Fourier transform technique, Journal of Applied Geophysics, 46, 159–174.

Mikhailov,V., G. Pajot, M.Diament, and A. Price, (2007), Tensor deconvolution: A method to locate equivalent sources from full tensor gravity data, Geophysics, 72, I61–I69, doi: 10.1190/1.2749317.

Pedersen, L. B., and T. M. Rasmussen, (1990), The gradient tensor of potential field anomalies:Some implications on data collection and data processing of maps, Geophysics, 55, 1558-1566.

Saad, A.H., (2006) Understanding gravity gradients—a tutorial, SaadGeoConsulting, Richmond, Texas, USA, The Leading Edge, 2006, 942-949.

Yuan, Y., and Q. YU, (2014), Edge Detection in Potential-Field Gradient Tensor Data by Use of Improved Horizontal Analytical Signal Methods, Pure Appl. Geophysics, doi: 10.1007/s00024-014-0880-1

Full gravity gradient tensor of Pyramid model